PFC/JA-88-01

# RESONANT OPERATION OF THE CROSS-FIELD FREE ELECTRON LASER: KINETIC AND FLUID EQUILIBRIA

G.L. Johnston
F. Hartemann†
R.C. Davidson
G. Bekefi

January, 1988

Plasma Fusion Center
Massachusetts Institute of Technology
Cambridge, MA 02139

†Permanent Address: Thomson-CSF, 2 Latecoere, B.P. 23, 78140, Velizy-Villacoublay, France.

# Resonant Operation of the Cross-field Free Electron Laser: Kinetic and Fluid Equilibria

*G.L. Johnston, F. Hartemann†, R.C. Davidson, and G. Bekefi*

*Plasma Fusion Center, Massachusetts Institute of Technology, Cambridge, Massachusetts 02139*

## ABSTRACT

Multiple-scale perturbation theory is used to obtain periodic orbits of relativistic electrons in the external electric and magnetic fields of a planar cross-field free electron laser (FEL) operating near the fundamental resonance. The condition for this resonance is $2\gamma_0 k_w v_0 \approx (eB_0/\gamma_0 m_0)(1+a_w^2)^{-1/2}$, where $k_w$ is the wavenumber of the magnetic wiggler field, $v_0 = E_0/B_0$ is the electron drift speed in the crossed uniform electric and magnetic fields, $\gamma_0 = (1 - v_0^2/c^2)^{-1/2}$ is the relativistic factor associated with the Lorentz transformation between the laboratory frame and the drift frame, $m_0$ is the rest mass of the electron, $a_w = 2^{-1/2}(eB_w/m_0 ck_w)$ is the normalized r.m.s. vector potential of the wiggler field, and $B_w$ is the magnitude of the wiggler field. The orbits are expressed in an approximate form suitable for use in linearized Vlasov stability analysis and are used to obtain Vlasov distribution functions which correspond to kinetic equilibria that are uniform and nonuniform (across the anode-cathode gap). Appropriate moments of these distribution functions yield corresponding fluid equilibria. These equilibria are developed as a basis for a linear stability analysis of the cross-field FEL operating near the fundamental resonance.

---

† *Present address: Thomson-CSF, 2 Latecoere, B.P. 23, 78140, Velizy-Villacoublay, France*

## 1. Introduction

The cross-field free electron laser (FEL) is a generator of coherent electromagnetic radiation in which a tenuous relativistic electron beam propagates in an anode-cathode gap that contains a combination of external fields similar to the external fields of a magnetron and the field of a magnetic wiggler. The configuration of the device may be coaxial or planar. For the sake of simplicity, a planar configuration will be considered in this work. (See Figure 1.) The magnetron fields are crossed electric and magnetic fields, $\vec{E}_0^{\ell}$ and $\vec{B}_0^{\ell}$. (The superscript $\ell$ denotes the laboratory frame. It is added because most of the analysis presented in this paper is carried out in the $\vec{E}_0^{\ell} \times \vec{B}_0^{\ell}$ drift frame.) The planar anode and cathode, which are not indicated in the figure, are perpendicular to the electric field. The axial direction of the anode-cathode gap is perpendicular to the electric and magnetic fields. The wiggler field $\vec{B}_w^{\ell}$ is a planar magnetic field whose polarization is parallel to the electric field $\vec{E}_0^{\ell}$ and which varies harmonically in the axial direction of the anode-cathode gap with spatial period $2\pi/k_w$, where $k_w$ is the wiggler wavenumber.

The dominant motion of electrons in the external fields is a drift of velocity $\vec{v}_0 = \vec{E}_0^{\ell} \times \vec{B}_0^{\ell}/B_0^2$, where $B_0$ is the magnitude of $\vec{B}_0^{\ell}$. In some of the theoretical work concerning cross-field FEL's published to date,[1-3] the motion of electrons in the external fields relative to the $\vec{E}_0^{\ell} \times \vec{B}_0^{\ell}$ drift is assumed to be mainly perpendicular to the plane of the wiggler, as in the case of a conventional FEL with planar wiggler. (This is the direction parallel to the uniform magnetic field $\vec{B}_0^{\ell}$.)

Examination of the equations of motion of a relativistic electron in the external fields discloses the existence of a series of nonlinear resonances. They may be described as occur-

ring between twice the wiggler-induced frequency and the gyro-frequency in the uniform magnetic field, both expressed in the drift frame of reference. The condition for the fundamental resonance is given in the limit of a weak wiggler by the approximate equality $2\gamma_0 k_w v_0 \approx eB_0/\gamma_0 m_0$,[4] where $v_0 = E_0/B_0$ is the electron drift speed in the crossed uniform electric and magnetic fields, $\gamma_0 = (1 - v_0^2/c^2)^{-1/2}$ is the relativistic factor associated with the Lorentz transformation between the laboratory frame and the drift frame, and $m_0$ is the rest mass of the electron. Near the fundamental resonance, the electron motion is primarily in the plane of the wiggler. Several theoretical and experimental[4-8] investigations have explored this resonance and the generation of electromagnetic radiation associated with instability occurring under fundamental resonance conditions. Heretofore, electron motion in the external fields near the fundamental resonance has been obtained from a nonresonant linear analysis, with the amplitude of the motion treated as a specified parameter. This procedure is incomplete, although it is not objectionable as far as it goes because the functional form of very weakly nonlinear motion near the resonance is the same as that of linear nonresonant motion. In both cases, the motion is driven at the frequency $\omega_d = 2\gamma_0 k_w v_0$ and there is a phase constant which depends on the mean electron position. The amplitude of the motion, however, depends on the extent to which the resonance condition is satisfied. Near resonance, the amplitude is strongly enhanced. This is extremely significant for the linear stability analysis because the growth rate of the instability is proportional to the amplitude of the motion.

The ultimate objective of this work is to develop kinetic and fluid equilibria which are valid for conditions near the fundamental resonance. These equilibria provide the

basis for a linear stability analysis of the cross-field FEL under such conditions, which will be presented in a subsequent paper. The process for obtaining the equilibria is the following. Multiple-scale perturbation theory is used to obtain an analytic approximation to weakly nonlinear, periodic, single-particle motion near the fundamental resonance. In the process of deriving the approximate motion it is found that, in the case of finite wiggler amplitude, the correct resonance condition is $2\gamma_0 k_w v_0 \approx (eB_0/\gamma_0 m_0)(1+a_w^2)^{-1/2}$, where $a_w = 2^{-1/2}(eB_w/m_0 c k_w)$ is the normalized r.m.s. vector potential of the wiggler field and $B_w$ is the magnitude of the wiggler field. The amplitude of the motion, treated in previous work as a specified parameter, is determined by the solution of a cubic equation. The orbits are placed in an approximate form suitable for use in linearized Vlasov stability analysis and are used to obtain Vlasov distribution functions which correspond to kinetic equilibria that are uniform and nonuniform (across the anode-cathode gap). Appropriate moments of these distribution functions yield corresponding fluid equilibria.

In Section 2 the external fields and the single-particle equations of motion are expressed in the $\vec{E}_0^{\ell} \times \vec{B}_0^{\ell}$ drift frame. Two of the component equations of motion are integrated directly to yield exact invariants. They are used, in combination with the remaining component equation of motion, to obtain a second-order differential equation for the component of electron position in the axial direction of the anode-cathode gap as a function of time. This equation is referred to as the exact combined differential equation. Because of the complexity of this equation, exact analytic solutions are almost certainly not available. In Section 3 an approximation to the exact combined differential equation is obtained. It has the form of a weakly nonlinear oscillator that is weakly driven by a wave-harmonic

excitation. It is referred to as the approximate combined differential equation. Because of the spatial dependence of the wave-harmonic excitation, it is a more complicated equation with a more extensive structure of resonances than the corresponding equation driven by a time-harmonic excitation. In Section 4 multiple-scale perturbation theory is used to obtain lowest-order periodic solutions of the approximate combined differential equation near the fundamental resonance. In Section 5 the orbits which have been obtained are placed in an approximate form suitable for use in linearized Vlasov stability analysis. They are used to obtain Vlasov distribution functions which correspond to kinetic equilibria that are uniform and nonuniform (across the anode-cathode gap). Appropriate moments of these distribution functions yield corresponding fluid equilibria. In Section 6 the results of this work are summarized.

## 2. Equations of motion and invariants in the $\vec{E}_0^\ell \times \vec{B}_0^\ell$ frame

In this section the external fields and the single-particle equations of motion are expressed in the $\vec{E}_0^\ell \times \vec{B}_0^\ell$ drift frame. Two of the component equations of motion are integrated directly to yield exact invariants. They are used, in combination with the remaining components equation of motion, to obtain a second-order differential equation for the component of electron position in the axial direction of the anode-cathode gap as a function of time. This equation is referred to as the exact combined differential equation. Because of the complexity of this equation, exact analytic solutions are almost certainly not available.

There are two motivations for transforming to the drift frame: first, to remove the static electric field; and second, to satisfy the condition that the motion is non-relativistic for typical velocities, *i.e.*, $v^2/c^2 \ll 1$.

The geometry and external fields of the system are described by Figure 1, which also indicates the Lorentz transformation between the laboratory frame, denoted by $S_\ell$, and the $\vec{E}_0^\ell \times \vec{B}_0^\ell$ drift frame, denoted by $S$. In the laboratory frame, the external fields are

$$\vec{E}_0^\ell = E_0 \hat{e}_x, \qquad \vec{B}_0^\ell = B_0 \hat{e}_y, \tag{1-a}$$

and

$$\vec{B}_w^\ell = B_w \cos(k_w z_\ell) \hat{e}_x. \tag{1-b}$$

Here $z_\ell$ is the z-component of position in the laboratory frame. The velocity of the $S$ frame with respect to the $S_\ell$ frame is

$$\vec{v}_0 = v_0 \hat{e}_z, \tag{2}$$

where $v_0 = E_0/B_0$. (Rationalized MKS units are used in this paper.) The relativistic factor $\gamma_0$ associated with the Lorentz transformation between the laboratory frame and the drift frame is given by

$$\gamma_0 = (1 - v_0^2/c^2)^{-1/2}. \tag{3}$$

The relation between $z_\ell$ and the z-component of position, z, and the time, t, in the drift frame, is given by

$$z_\ell = \gamma_0 (z + v_0 t). \tag{4}$$

The Lorentz transformation equations for the electric and magnetic fields in the drift frame are

$$\vec{E} = \gamma_0 (\vec{E}^\ell + \vec{v}_0 \times \vec{B}^\ell)$$

and

$$\vec{B} = \gamma_0 (\vec{B}^\ell - c^{-2} \vec{v}_0 \times \vec{E}^\ell),$$

where $\vec{E}^{\ell} = \vec{E}_0^{\ell}$ and $\vec{B}^{\ell} = \vec{B}_0^{\ell} + \vec{B}_w^{\ell}$. Explicit expressions for $\vec{E}$ and $\vec{B}$ are

$$\vec{E} = \gamma_0 v_0 B_w \cos[\gamma_0 k_w (z + v_0 t)]\hat{e}_y \tag{5–a}$$

and

$$\vec{B} = \gamma_0 B_w \cos[\gamma_0 k_w (z + v_0 t)]\hat{e}_x + \gamma_0^{-1} B_0 \hat{e}_y. \tag{5–b}$$

(See Figure 1. There, but not in the text, the uniform and nonuniform, time-dependent parts of the magnetic field $\vec{B}$ of (5–b) have been denoted for the sake of clarity by $\vec{B}_0$ and $\vec{B}_w$, respectively.)

The single-particle equations of motion in the drift frame are

$$\frac{d\vec{p}}{dt} = -e(\vec{E} + \vec{v} \times \vec{B}) \tag{6}$$

and

$$\frac{d\gamma}{dt} = -\frac{e}{m_0 c^2} \vec{v} \cdot \vec{E}, \tag{7}$$

where $\vec{E}$ and $\vec{B}$ are given by (5). The relation between the momentum $\vec{p}$ and the velocity $\vec{v}$ is

$$\vec{p} = \gamma m_0 \vec{v} \tag{8}$$

where

$$\gamma = (1 - v^2/c^2)^{-1/2} = (1 + p^2/m_0^2 c^2)^{1/2}. \tag{9}$$

The cartesian component equations of motion in the drift frame are

$$\frac{dp_x}{dt} = eB_0 \gamma_0^{-1} v_z, \tag{10–a}$$

$$\frac{dp_y}{dt} = -eB_w \gamma_0 (v_0 + v_z) \cos[\gamma_0 k_w (z + v_0 t)], \tag{10–b}$$

$$\frac{dp_z}{dt} = -eB_0\gamma_0^{-1}v_x + eB_w\gamma_0 v_y \cos[\gamma_0 k_w(z + v_0 t)], \tag{10-c}$$

and

$$\frac{d\gamma}{dt} = -\frac{e}{m_0 c}v_y\gamma_0\left(\frac{v_0}{c}\right)B_w \cos[\gamma_0 k_w(z + v_0 t)]. \tag{10-d}$$

Eqs. (10a) and (10b) can be integrated at once to give the exact invariant equations

$$p_x - eB_0\gamma_0^{-1}z = C_x \tag{11}$$

and

$$p_y + eB_w k_w^{-1}\sin[\gamma_0 k_w(z + v_0 t)] = C_y. \tag{12}$$

A third invariant can be obtained by eliminating the quantity $eB_w\gamma_0 v_y \cos[\gamma_0 k_w(z + v_0 t)]$ between (10–c) and (10–d) and integrating the resulting equation. This invariant is not required for the derivation of the exact combined differential equation. The appropriate choice of constants is $C_x = -eB_0\gamma_0^{-1}z_0$ and $C_y = 0$. The choice of $C_x$, which is merely a matter of notation, reflects the expectation that the motion is oscillatory. As will be seen more clearly below, $z_0$ is a guiding-center coordinate. The choice of $C_y$ is motivated by the requirement that the motion not contain a secular drift. The invariant equations can be used, in combination with (9), to obtain an expression for $\gamma$ as a function of $z$, $v_z$ and $t$. The result is

$$\frac{1}{\gamma^2} = \frac{(1 - c^{-2}v_z^2)}{[1 + c^{-2}(\hat{v}_x^2 + \hat{v}_y^2)]}. \tag{13}$$

In this expression the quantities $\hat{v}_x$ and $\hat{v}_y$ are given by the expressions

$$\hat{v}_x = \gamma v_x = \omega_0(z - z_0), \tag{14}$$

and

$$\hat{v}_y = \gamma v_y = -2^{1/2}a_w c \sin[\gamma_0 k_w(z + v_0 t)], \tag{15}$$

where

$$\omega_0 = eB_0/\gamma_0 m_0 \tag{16}$$

is the gyro-frequency in the uniform magnetic field and

$$a_w = 2^{-1/2}(eB_w/m_0 ck_w) \tag{17}$$

is the normalized r.m.s. vector potential of the wiggler field. Eqs. (14) and (15) are alternative expressions of the invariant equations, (11) and (12), with the particular choice of constants stated above.

In order to obtain a second-order differential equation which describes the dynamics of single-particle motion, it is necessary to express the z-component equation of motion (10–c) in terms of $dv_z/dt$ instead of $dp_z/dt$. This is accomplished by use of (10–d). The result is

$$\frac{dv_z}{dt} = -\frac{\omega_0}{\gamma}\left\{v_x - \frac{B_w}{B_0}\gamma_0^2\left(1 + \frac{v_0 v_z}{c^2}\right)v_y \cos[\gamma_0 k_w(z + v_0 t)]\right\}. \tag{18}$$

Eq. (18) is transformed into the desired equation by expressing $v_x$ and $v_y$ in terms of $z$, $v_z$ and $t$ through use of (14) and (15) and introduction of the identity $v_z = dz/dt$. The result is

$$\frac{d^2 z}{dt^2} + \frac{\omega_0^2}{\gamma^2}(z - z_0) = -\frac{1}{2}\frac{B_w^2 \omega_0^2 \gamma_0^3}{B_0^2 k_w \gamma^2}\left(1 + \frac{v_0 v_z}{c^2}\right)\sin[2\gamma_0 k_w(z + v_0 t)]. \tag{19}$$

Eq. (19), supplemented by (13)–(15) and the identity $v_z = dz/dt$, is the desired second-order differential equation for z as a function of t. Henceforth it will be referred to as the exact combined differential equation. It is an equation of the form

$$\frac{d^2 z}{dt^2} = F\left(z, \frac{dz}{dt}, t\right). \tag{20}$$

Solutions of this equation which are acceptable as a basis for the linear stability analysis of the cross-field FEL (not necessarily operating in the resonant mode) must exhibit suitable periodicity when transformed into the laboratory frame. It is necessary that deviations of $z_\ell = z_\ell(t_\ell)$ from uniform motion with drift speed $v_0$ be periodic with the wiggler period or an integral submultiple of it. A precise statement of this requirement is the following: the quantity $\{[z_\ell(t_\ell) - z_\ell(0)] - v_0 t_\ell\}$ is required to be a periodic function of $t_\ell$ with period $T_n^\ell = L_n^\ell / v_0$, where $L_n^\ell = 2\pi/nk_w$, $n = 1, 2, 3, \cdots$, and $z_\ell(0)$ is unrestricted. The transformation of this requirement to the drift frame yields a condition which solutions of the exact combined differential equation must satisfy in order to be acceptable as a basis for linear stability analysis of the cross-field FEL. The Lorentz transformation from the laboratory frame to the drift frame is

$$x = x_\ell, \qquad y = y_\ell, \tag{21}$$

$$z = \gamma_0(z_\ell - v_0 t_\ell), \tag{22}$$

and

$$t = \gamma_0(t_\ell - v_0 z_\ell / c^2). \tag{23}$$

A laboratory frame interval $(L_n^\ell, T_n^\ell)$ corresponds to a drift frame interval $(L_n, T_n)$, where $L_n = 0$ and $T_n = T_n^\ell/\gamma_0 = 2\pi/n\gamma_0 k_w v_0$. Therefore, solutions of the exact combined differential equation which are acceptable for the linear stability analysis of the cross-field FEL must be periodic with period $2\pi/\omega_n$, where

$$\omega_n = n\gamma_0 k_w v_0 \quad , \quad n = 1, 2, 3, \cdots. \tag{24}$$

An approximation to the exact combined differential equation which is a weakly nonlinear oscillator that is weakly driven by a wave-harmonic excitation will be developed in

the Section 3. The resonance conditions for this equation will be shown in Section 4 to be [see (49)]

$$\omega_d \approx m\omega_0^* \quad , \quad m = 1, 2, 3, \cdots,$$

where [(43)]

$$\omega_d = 2\gamma_0 k_w v_0$$

is the Lorentz transformed frequency of the effective driving force of (19) in the limit of small-amplitude excitation, and [(36)]

$$\omega_0^* = \omega_0/(1 + a_w^2)^{1/2}$$

is the harmonic frequency of (17) in the limit of small-amplitude excitation. It is close to the frequency of weakly nonlinear resonant solutions of the equation.

It is necessary that the frequency of weakly nonlinear resonant solutions be close to a frequency which is allowable under the periodicity condition, i.e.,

$$\omega_n \approx \omega_0^*. \tag{25}$$

Examination of the periodicity condition (24) and the resonance condition [see (49)] discloses the allowable combinations of values of $m$ and $n$. The condition which results is

$$mn = 2. \tag{26}$$

This relation shows that, among resonant solutions, only the fundamental resonance ($m = 1$) and the first subharmonic resonance ($m = 2$) are acceptable as a basis for the linear stability analysis of the cross-field FEL. The spatial periodicity in the laboratory frame of

the fundamental resonance ( $m = 1$ ) is the first integral subharmonic of the wiggler period ( $L_2^\ell = \pi/k_w$ ). The spatial periodicity in the laboratory frame of the first subharmonic resonance ( $m = 2$ ) is the wiggler period ( $L_1^\ell = 2\pi/k_w$ ).

## 3. Approximate combined differential equation

In this section an approximation to the exact combined differential equation is obtained. It has the form of a weakly nonlinear oscillator that is weakly driven by a wave-harmonic excitation. It is referred to as the approximate combined differential equation. Because of the spatial dependence of the wave-harmonic excitation, it is a more complicated equation with a more extensive structure of resonances than the corresponding equation driven by a time-harmonic excitation.

The paradigmatic equation of a weakly nonlinear oscillator that is weakly driven near resonance by a time-harmonic excitation is

$$\frac{d^2x}{dt^2} + x + \epsilon N\left(x, \frac{dx}{dt}\right) = \epsilon f \sin[(1 + \epsilon\Omega)t + \chi], \tag{27}$$

In this equation $\epsilon$ is a smallness parameter ($\epsilon^2 \ll 1$), and $f$ and $\Omega$ are constants of order one; $N$ is a function of order one; $\chi$ is a phase constant. Two examples of this paradigmatic equation are the time-harmonically excited Duffing equation,

$$\frac{d^2x}{dt^2} + x + \epsilon x^3 = \epsilon f \sin[(1 + \epsilon\Omega)t + \chi], \tag{28}$$

and the time-harmonically excited van der Pol equation,

$$\frac{d^2x}{dt^2} + x = \epsilon(1 - x^2)\frac{dx}{dt} + \epsilon f \sin[(1 + \epsilon\Omega)t + \chi]. \tag{29}$$

Multiple-scale perturbation theory is capable of providing approximate analytic solutions of these and similar equations, including the approximate combined differential equation, near conditions of resonance.

An obvious first step in the process of approximating the exact combined differential equation is the introduction of the transformed dependent variable

$$\Delta z = (z - z_0). \tag{30}$$

The significance of the constant $z_0$ as a guiding-center coordinate is now clear.

The next step is the development of an approximation of the second term on the left-hand side of (19), $\omega_0^2 \gamma^{-2} \Delta z$, which includes lowest-order resonant nonlinear terms. Examination of (13) shows that, if $v^2/c^2$ and $a_w^2$ are much less than one, then $\gamma^{-2}$ can be approximated by the expansion

$$\gamma^{-2} = 1 - [c^{-2}(\hat{v}_x^2 + v_z^2)] - c^{-2}\hat{v}_y^2 + \cdots, \tag{31}$$

where $\hat{v}_x$ and $\hat{v}_y$ are given by (14) and (15), respectively. Because there is a practical possibility that $a_w^2$ may *not* be much less than one, the quantity $c^{-2}\hat{v}_y^2$, which formally is of higher order in (31), may in fact be of lowest order. An alternative approximation to $\gamma^{-2}$ is therefore required.

In order to see what that approximation should be, note that the quantity $c^{-2}\hat{v}_y^2$ can be expressed as

$$c^{-2}\hat{v}_y^2 = a_w^2\{1 - \cos[2\gamma_0 k_w(z + v_0 t)]\}. \tag{32}$$

Consider multiplication of (19) term-by-term by the denominator of the expression for $\gamma^{-2}$ given in (13). The resulting equation contains a term

$$-a_w^2 \cos[2\gamma_0 k_w(z + v_0 t)] \frac{d^2 z}{dt^2}.$$

This term is nonresonant (at the second harmonic of the resonant response) and, accordingly, can be neglected. Therefore $\gamma^{-2}$ can be expressed by the approximate relation

$$\frac{1}{\gamma^2} \approx \frac{(1 - c^{-2}v_z^2)}{[(1 + a_w^2) + c^{-2}\hat{v}_x^2]}. \tag{33}$$

If $(1 + a_w^2)^{-1}c^{-2}\hat{v}_x^2 \ll 1$ and $c^{-2}v_z^2 \ll 1$, then $\gamma^{-2}$ can be approximated by

$$\gamma^{-2} \approx (1 + a_w^2)^{-1}[1 - (1 + a_w^2)^{-1}c^{-2}\hat{v}_x^2 - c^{-2}v_z^2 + \cdots]. \tag{34}$$

Making use of (14) and the relation $v_z = d\Delta z/dt$, it is now possible to give the desired approximation of $\omega_0^2\gamma^{-2}\Delta z$, namely

$$\omega_0^2 \frac{1}{\gamma^2}\Delta z \approx \omega_0^{*2}\left[1 - \frac{1}{c^2}\omega_0^{*2}(\Delta z)^2 - \frac{1}{c^2}\left(\frac{d\Delta z}{dt}\right)^2 + \cdots\right]\Delta z, \tag{35}$$

where

$$\omega_0^* = \omega_0/(1 + a_w^2)^{1/2} \tag{36}$$

is the harmonic frequency of (19) in the limit of small-amplitude excitation. The second and third terms on the right-hand side of (35) give rise to cubic nonlinearities, which contain resonant contributions.

It is necessary for the application of multiple-scale perturbation theory to express the approximate equation in terms of dimensionless dependent and independent variables and a smallness parameter. Examination of (35) permits the determinination of those quantities. The dimensionless dependent variable is

$$\widetilde{\Delta z} \equiv \frac{\Delta z}{A}, \tag{37}$$

where $A$ is a characteristic amplitude of the motion. The dimensionless independent variable is

$$\tilde{t} \equiv \omega_0^* t. \tag{38}$$

The smallness parameter is

$$\epsilon = \left(\frac{\omega_0^* A}{c}\right)^2. \tag{39}$$

Note that the neglected terms on the right-hand side of (35) are of order $\epsilon^2$.

The next steps in the process of approximating the exact combined differential equation involve the right-hand side of (19): the neglect of $v_0 v_z/c^2$ compared with one and the approximation of $\gamma^{-2}$ by $(1+a_w^2)^{-1}$. The former approximation is justified because it contributes a non-resonant term to the equation, which, incidentally, is of order $\epsilon^{1/2}$. The validity of the latter approximation is predicated on the assumption that the magnitude of the right-hand side of the equation is of order $\epsilon$. As was shown above, the magnitude of the difference between $\gamma^{-2}$ and $(1+a_w^2)^{-1}$ is of order $\epsilon$.

The equation which results from the introduction into (19) of the approximations which have been discussed up to this point and the use of the dimensionless variables and the smallness parameter is

$$\frac{d^2\widetilde{\Delta z}}{d\tilde{t}^2} + \left\{1 - \epsilon\left[(\widetilde{\Delta z})^2 + \left(\frac{d\widetilde{\Delta z}}{d\tilde{t}}\right)^2\right]\right\}\widetilde{\Delta z} = -\epsilon f \sin(\alpha\widetilde{\Delta z} + \tilde{\omega}_d\tilde{t} + \tilde{t}_0), \tag{40}$$

In this equation the quantities $f$, $\alpha$, $\tilde{\omega}_d$, and $\tilde{t}_0$ are given by the relations

$$\epsilon f = \frac{1}{2}\frac{B_w^2}{B_0^2}\frac{\gamma_0^3}{k_w A}, \tag{41}$$

where $f$ is assumed to be of order one,

$$\alpha = 2\gamma_0 k_w A, \tag{42}$$

$\tilde{\omega}_d = \omega_d/\omega_0^*$, where

$$\omega_d = 2\gamma_0 k_w v_0, \tag{43}$$

is the doppler-shifted frequency of the effective driving force of (19) in the limit of small-amplitude excitation, and

$$\tilde{t}_0 = 2\gamma_0 k_w z_0. \tag{44}$$

This is a weakly nonlinear oscillator that is weakly driven by a wave-harmonic excitation. It is a more complicated equation with a more extensive structure of resonances than the corresponding equation driven by a time-harmonic excitation.

## 4. Multiple-Scale Solution of Approximate Equation

In this section multiple-scale perturbation theory is used to obtain lowest-order periodic solutions of the approximate combined differential equation near the fundamental resonance.

The two-variable expansion of $\widetilde{\Delta z}$ has the form

$$\widetilde{\Delta z} = u_0(T_0, T_1) + \epsilon u_1(T_0, T_1) + \cdots, \tag{45}$$

where

$$T_0 = \tilde{t} \tag{46}$$

and

$$T_1 = \epsilon\tilde{t} \tag{47}$$

are the fast and slow independent variables, respectively. The derivative with respect to $\tilde{t}$ is expressed in terms of derivatives with respect to $T_0$ and $T_1$ by

$$\frac{d}{d\tilde{t}} = \frac{\partial}{\partial T_1} + \epsilon\frac{\partial}{\partial T_1}. \tag{48}$$

It will be shown below [see the discussion following (55)] that the resonant conditions are given by the equation

$$\tilde{\omega}_d (= \omega_d/\omega_0^*) = m + \epsilon\sigma, \tag{49}$$

where $\sigma$ is of order one and the values of $m$ which correspond to resonance are $1, 2, 3, \cdots$.

Substitution of the expressions for $\widetilde{\Delta z}$ [(45)] and $\tilde{\omega}_d$ [(49)] into the approximate combined differential equation (40), use of (46)–(48), and segregation of terms which contain different powers of $\epsilon$, give the following equations at $O(1)$ and $O(\epsilon)$, respectively:

$$\left(\frac{\partial^2}{\partial T_0^2} + 1\right) u_0 = 0 \tag{50}$$

and

$$\left(\frac{\partial^2}{\partial T_0^2} + 1\right) u_1 = -2\frac{\partial^2 u_0}{\partial T_1 \partial T_0} + u_0^3 + \left(\frac{\partial u_0}{\partial T_0}\right)^2 u_0 - f\sin(\alpha u_0 + mT_0 + \sigma T_1 + \tilde{t}_0). \tag{51}$$

The general solution of (51) is

$$u_0 = U(T_1)\sin[T_0 + \phi(T_1)], \tag{52}$$

where $U$ and $\phi$ are, respectively, the slowly varying amplitude and phase. Substitution of this expression for $u_0$ into the right-hand side of (51) yields the equation

$$\begin{aligned}\left(\frac{\partial^2}{\partial T_0^2} + 1\right) u_1 = &-2\frac{dU}{dT_1}\cos(T_0 + \phi) + \left(2U\frac{d\phi}{dT_1} + U^3\right)\sin(T_0 + \phi) \\ &- f\sin\{[\alpha U\sin(T_0 + \phi) + m(T_0 + \phi)] + \psi_m\}.\end{aligned} \tag{53}$$

In this equation

$$\psi_m = \sigma T_1 - m\phi + \tilde{t}_0 \tag{54}$$

is the transformed slowly-varying phase. The Fourier expansion of the right-hand side of (53) in the fast independent variable contains terms which are proportional to $\exp[\pm i(T_0 + \phi)]$. These terms drive the left-hand side of the equation resonantly and therefore produce secular terms in $u_1$ because the coefficients of $\exp[\pm i(T_0 + \phi)]$ are functions of $T_1$ only. In order that $u_1/u_0$ be bounded for all $T_0$, it is necessary and sufficient that the coefficient of $\exp[i(T_0 + \phi)]$ on the right-hand side of (53) vanish. This is the essence of the resonant multiple-scale theory. Fourier expansion of the last term on the right-hand side of (53) is effected by means of the Bessel-function identity $\exp(iq\sin\eta) = \sum_{\ell=-\infty}^{\infty} J_\ell(q)\exp(i\ell q)$. The result is

$$-f\sin\{\cdots\} = \frac{1}{2}ife^{i\psi_m}\sum_{\ell=-\infty}^{\infty} J_\ell(\alpha U)e^{i(\ell+m)(T_0+\phi)} - \frac{1}{2}ife^{-i\psi_m}\sum_{\ell=-\infty}^{\infty} J_\ell(\alpha U)e^{-i(\ell+m)(T_0+\phi)}. \tag{55}$$

In the first series on the right-hand side of (55), the desired term corresponds to $\ell + m = 1$. In the second series, the desired term corresponds to $\ell + m = -1$. Examination of these conditions and (49) shows that, as asserted above, the values of m which correspond to resonance are $m = 1, 2, 3, \cdots$. The value $m = 1$ corresponds to the fundamental resonance. The condition for the exclusion of secular behavior of $u_1$ which is obtained from (53) with the aid of (55) is

$$\frac{dU}{dT_1} + i\left(U\frac{d\phi}{dT_1} + \frac{1}{2}U^3\right) - \frac{1}{2}ife^{i\psi_m}J_{1-m}(\alpha U) + \frac{1}{2}ife^{-i\psi_m}J_{-1-m}(\alpha U) = 0. \tag{56}$$

Separation of the real and imaginary parts of this equation, use of the Bessel-function identities $2nJ_n = x(J_{n-1} + J_{n+1})$, $2J_n' = J_{n-1} - J_{n+1}$, and $J_{-m} = (-)^m J_m$, and (54),

yields the following pair of equations for the evolution of $U(T_1)$ and $\psi_m(T_1)$:

$$\frac{dU}{dT_1} + (-)^{m+1} fm \frac{J_m(\alpha U)}{\alpha U} \sin\psi_m = 0 \tag{57}$$

and

$$U\frac{d\psi_m}{dT_1} - \sigma U - \frac{1}{2}mU^3 + (-)^{m+1} fm J'_m(\alpha U)\cos\psi_m = 0. \tag{58}$$

Davidson[9] has recently reduced the solution of the coupled set of equations (57) and (58) to quadrature. This is accomplished by means of an exact invariant of the set. The evolution of $U$ is determined by an 'energy' conservation equation

$$\frac{1}{2}\left(\frac{dU^2}{dT_1}\right)^2 + W(U^2) = 0,$$

where $W(U^2)$ is an effective potential. The evolution of $U$ in the general case corresponds to trapped motion of an equivalent particle between the turning points of the effective potential. The stationary solutions of (57) and (58), which are obtained by setting the derivatives with respect to $T_1$ equal to zero, correspond to 'motion' at the bottom of the effective potential.

In the case of the fundamental resonance, $m = 1$, the set of equations (57) and (58) assumes the form

$$\frac{dU}{dT_1} + f\frac{J_1(\alpha U)}{\alpha U} \sin\psi_1 = 0 \tag{59}$$

and

$$U\frac{d\psi_1}{dT_1} - \sigma U - \frac{1}{2}U^3 + fJ'_1(\alpha U)\cos\psi_1 = 0. \tag{60}$$

Since $m = 1$ and $\epsilon|\sigma| \ll 1$, it follows from (49) that $\omega_0^* \approx \omega_d$. By using this approximate identity, the definitions of $\epsilon$ [(39)], $\alpha$ [(42)], and $\omega_d$ [(43)], and the condition $v_0 \approx c$, it

can be shown that

$$\alpha \approx \epsilon^{1/2}. \tag{61}$$

In the case of periodic solutions of (40), such as those sought here, the magnitude of $U$ is a constant and can be chosen for convenience to be equal to one. (This is possible because $A$ was introduced [in (37)] as an arbitrary constant.) These observations yield the approximate identity $\alpha U \approx \epsilon^{1/2}$ for the value of the argument of the Bessel functions in (59) and (60). The use of this approximate identity and the Bessel-function identity

$$J_1(x) = \frac{1}{2}x - \frac{(\frac{1}{2}x)^3}{1^2 \cdot 2} + \frac{(\frac{1}{2}x)^5}{1^2 \cdot 2^2 \cdot 3} - \cdots$$

makes it possible to approximate the equations (59) and (60) with an error of order $\epsilon$ by the equations

$$\frac{dU}{dT_1} + \frac{1}{2} f \sin\psi_1 = 0 \tag{62}$$

and

$$U\frac{d\psi_1}{dT_1} - \sigma U - \frac{1}{2}U^3 + \frac{1}{2} f \cos\psi_1 = 0. \tag{63}$$

The stationary solutions of (62) and (63) correspond to lowest-order periodic solutions of the approximate combined differential equation (40) near the fundamental resonance $\omega_d \approx \omega_0^*$. They are obtained by setting $dU/dT_1$ and $d\psi_1/dT_1$ equal to zero. The equations which result are

$$(1/2) f \sin\psi_{10} = 0 \tag{64}$$

and

$$\sigma U_0 + (1/2)U_0^3 - (1/2) f \cos\psi_{10} = 0, \tag{65}$$

where $U_0$ and $\psi_{10}$ are the stationary values of $U$ and $\psi_1$. Eq. (64) is satisfied by the values

$$\psi_{10} = \begin{cases} 0 \\ \pi \end{cases}, \tag{66}$$

which implies

$$\cos\psi_{10} = \pm 1. \tag{67}$$

Substitution of these values of $\cos\psi_{10}$ into (65) yields the equation

$$\sigma U_0 + (1/2)U_0^3 \mp (1/2)f = 0, \tag{68}$$

which is a cubic equation in $U_0$. In order to gain insight into the behavior of the stationary solutions , it is convenient to solve (68) for $\sigma$ as a function of $U_0$ and $f$ $[\sigma = \sigma(U_0; f)]$:

$$\sigma = -\frac{1}{2}U_0^2 \pm \frac{1}{2}\frac{f}{U_0}. \tag{69}$$

Figure 2 gives a typical plot of $\sigma$ as a function of $U_0$ for fixed $f$. There are two branches of $\sigma(U_0; f)$, corresponding to $\psi_{10} = 0$ and $\psi_{10} = \pi$.

The stability of the motion described by the two branches of (69) is investigated by linearizing (62) and (63) about those branches. Let

$$U = U_0 + \Delta U \quad , \quad \psi = \psi_{10} + \Delta\psi_1. \tag{70}$$

Expansion of (62) and (63) in powers of $\Delta U$ and $\Delta\psi_1$ and retention of only linear terms yields

$$\frac{d\Delta U}{dT_1} \pm \frac{1}{2}f\Delta\psi_1 = 0 \tag{71}$$

and

$$\left(\sigma + \frac{3}{2}U_0^2\right)\Delta U - U_0\frac{d\Delta\psi_1}{dT_1} = 0. \tag{72}$$

If $\Delta a \propto \exp pT_1$ and $\Delta\psi \propto \exp pT_1$, then $p$ must satisfy the equation

$$p^2 = \mp\frac{1}{2}\frac{f}{U_0}\left(\sigma + \frac{3}{2}U_0^2\right). \tag{73}$$

The motion described by (62) and (63) is linearly stable around the stationary points $U = U_0$ and $\psi_1 = \psi_{10}$ if and only if $p^2 < 0$.

The entirety of the upper branch of $\sigma$ as a function of $U_0$ ($\psi_{10} = 0$) and that portion of the lower branch ($\psi_{10} = \pi$) with positive slope $[0 < U_0 < (f/2)^{1/3}]$ correspond to stable motion. These results are obtained in the following manner. Substitution of the expression for $\sigma$ as a function of $U_0$ from (69) into (73) yields the following equation for $p^2$ as a function of $U_0$:

$$p^2 = -\frac{1}{4}\frac{f^2}{U_0^2} \mp \frac{1}{2}fU_0. \tag{74}$$

Inspection of (74) for the upper branch ($\psi_{10} = 0$) shows that the entirety of that branch corresponds to stable motion. Inspection of (74) for the lower branch shows that $p^2$ is a monotonically increasing function of $U_0$. Small values of $U_0$ correspond to stability; large values of $U_0$ correspond to instability. The condition for marginal stability ($p^2 = 0$) is $U_0 = (f/2)^{1/3}$. The derivative of $\sigma(U_0; f)$ with respect to $U_0$ is given by the equation

$$\frac{d\sigma}{dU_0} = -U_0 \mp \frac{1}{2}\frac{f}{U_0^2}. \tag{75}$$

Inpection of this equation in the case of the lower branch indicates that the derivative is monotonically decreasing. It is positive for small values of $U_0$ and negative for large values of $U_0$. It vanishes for $U_0 = (f/2)^{1/3}$, which is also the condition for marginal stability of the lower branch. As asserted above, that portion of the lower branch of $\sigma(U_0; f)$ with positive slope $[0 < U_0 < (f/2)^{1/3}]$ corresponds to stable motion. See Figure 2.

It is now possible to determine the explicit form of the lowest-order periodic solutions of the approximate combined differential equation (40). Eqs. (39), (41), (49) (with $m = 1$), and (69) constitute a set of four equations in the five unknowns $A$, $\epsilon$, $f$, $\sigma$, and $U_0$. It is necessary to reduce the number of unknowns to the number of equations. In the case of periodic solutions of (40), such as those sought here, the magnitude of $U$ is a constant and can be chosen for convenience to be equal to one. This is possible because, as noted above, $A$ was introduced [in (37)] as an arbitrary constant. The use of (45)–(47), (49) (with $m = 1$), (52), (54), (66), and $U_0 = 1$ yields the following expression in lowest order for $\widetilde{\Delta z}$:

$$\widetilde{\Delta z} \approx \pm \sin(\tilde{\omega}_d \tilde{t} + \tilde{t}_0). \tag{76}$$

The only quantity which remains to be determined is $A$. The set of equations for the determination of $A$ consists of (39), (41), (49) (with $m = 1$), and [from (69), with $U_0 = 1$]

$$\sigma = -\frac{1}{2} \pm \frac{1}{2} f. \tag{77}$$

This set can be combined to give the following equation, which is a cubic in $\epsilon^{1/2}$:

$$\epsilon^{3/2} - 2\left(1 - \frac{\omega_d}{\omega_0^*}\right)\epsilon^{1/2} \mp \frac{1}{2}\frac{B_w^2}{B_0^2}\frac{\gamma_0^3 \omega_0^*}{k_w c} = 0. \tag{78}$$

Recall, from (37), that $\epsilon = (\omega_0^* A/c)^2$. Positive real solutions of (78) are required.

The use of (30), (37), (38), (44), (49) (with $m = 1$), and (76) yields the following expression for $z - z_0$:

$$z - z_0 = \pm A \sin(\omega_d t + 2\gamma_0 k_w z_0). \tag{79}$$

The components of the velocity of the single-particle motion are now obtained. The $z$-component is obtained by differentiation of (79) with respect to $t$. The result is

$$v_z = \pm \omega_d A \cos(\omega_d t + 2\gamma_0 k_w z_0). \tag{80}$$

The $x$-component of velocity is obtained from (14) and (79). The factor $\gamma^{-1}$ is replaced by its lowest-order approximation, $(1 + a_w^2)^{1/2}$, [see (33)] and use is made of (36). The result is

$$v_x = \pm\omega_0^* A \sin(\omega_d t + 2\gamma_0 k_w z_0). \tag{81}$$

This equation can be integrated to give

$$x - x_0 = \mp(\omega_0^*/\omega_d) A \cos(\omega_d t + 2\gamma_0 k_w z_0), \tag{82}$$

where $x_0$ is a guiding-center coordinate. The $y$-component of velocity is assumed to be negligible in cases of interest.

## 5. Vlasov and Fluid Equilibrium Results

In this section the orbits which have been obtained are expressed in an approximate form suitable for use in linearized Vlasov stability analysis. They are used to obtain Vlasov distribution functions which correspond to kinetic equilibria that are uniform and nonuniform (across the anode-cathode gap). Appropriate moments of these distribution functions yield corresponding fluid equilibria.

The orbits (79)–(82) are not in a functional form which is appropriate for linear Vlasov stability analysis. The appropriate functional form is

$$\vec{x}' = x'(\vec{x}, \vec{v}, t, t') \quad , \quad \vec{v}' = v'(\vec{x}, \vec{v}, t, t'). \tag{83}$$

Since the magnitude of $z - z_0$ is $A$, the error committed in replacing $z_0$ by $z$ in the argument of the trigonometric functions in (78)–(82) is of order $\epsilon^{1/2}$. [See (42) and (61).] With this approximation, it is possible to place the orbits in a form which is appropriate

for linear Vlasov stability analysis. The results are

$$z' - z = \pm A[\sin(\omega_d t' + 2\gamma_0 k_w z) - \sin(\omega_d t + 2\gamma_0 k_w z)], \tag{84}$$

$$v'_z - v_z = \pm\omega_d A[\cos(\omega_d t' + 2\gamma_0 k_w z) - \cos(\omega_d t + 2\gamma_0 k_w z)], \tag{85}$$

$$v'_x - v_x = \pm\omega_0^* A[\sin(\omega_d t' + 2\gamma_0 k_w z) - \sin(\omega_d t + 2\gamma_0 k_w z)], \tag{86}$$

and

$$x' - x = \mp(\omega_0^*/\omega_d)A[\cos(\omega_d t' + 2\gamma_0 k_w z) - \cos(\omega_d t + 2\gamma_0 k_w z)]. \tag{87}$$

Equilibrium Vlasov distribution functions are functions of invariants of single-particle motion in external fields. In the present case, appropriate invariants are obtained by expressing Eqs. (79)–(82) in the form of functions of dynamical variables set equal to zero. Cold equilibrium distribution functions contain suitable combinations of Dirac delta functions (more accurately *distributions*) whose arguments are these functions of dynamical variables.

The formal statement of the uniform-density Vlasov distribution function is

$$f_b^0(z, v_x, v_z, t) = n_0 \int_{-\infty}^{\infty} dz_0 \delta[z - z_0 \mp A\sin(\omega_d t + 2\gamma_0 k_w z_0)]$$
$$\times\, \delta[v_x \mp \omega_0^* A\sin(\omega_d t + 2\gamma_0 k_w z_0)]\delta[v_z \mp \omega_d A\cos(\omega_d t + 2\gamma_0 k_w z_0)], \tag{88}$$

where $n_0$ is a constant. This statement of the distribution function is not particularly useful because of the presence of the integral with respect to $z_0$. As in the case of the orbits, the error committed in replacing $z_0$ by $z$ in the argument of the trigonometric functions in (88) is of order $\epsilon^{1/2}$. With this approximation, the integral in (88) can be performed. The distribution function which results is

$$f_b^0(z, v_x, v_z, t) = n_0 \delta[v_x \mp \omega_0^* A\sin(\omega_d t + 2\gamma_0 k_w z)]\delta[v_z \mp \omega_d A\cos(\omega_d t + 2\gamma_0 k_w z)]. \tag{89}$$

The zeroth velocity moment of this distribution function yields the uniform fluid number density $N(z,t) = n_0$. The ratio of the first velocity moment to the number density is the fluid velocity of the cold-fluid equilibrium:

$$V_x(z,t) = \pm\omega_0^* A \sin(\omega_d t + 2\gamma_0 k_w z) \tag{90}$$

and

$$V_z(z,t) = \pm\omega_d A \cos(\omega_d t + 2\gamma_0 k_w z). \tag{91}$$

The formal statement of a Vlasov distribution function which corresponds to a simple (perhaps the simplest) kinetic equilibrium that is nonuniform (across the anode-cathode gap) is

$$f_b^0(x,z,v_x,v_z,t) = n_0 \int_{-d/2}^{d/2} dx_0 \delta[x - x_0 \pm (\omega_0^*/\omega_d) A \cos(\omega_d t + 2\gamma_0 k_w z)]$$
$$\times \delta[v_x \mp \omega_0^* A \sin(\omega_d t + 2\gamma_0 k_w z)]\delta[v_z \mp \omega_d A \cos(\omega_d t + 2\gamma_0 k_w z)]. \tag{92}$$

In presenting (92), an initial approximation corresponding to the progression from (88) to (89) has already been incorporated. Performance of the integral in (92) yields the result

$$f_b^0(x,z,v_x,v_z,t) = n_0\{\theta[x + d/2 \pm (\omega_0^*/\omega_d) A \cos(\omega_d t + 2\gamma_0 k_w z)]$$
$$- \theta[x - d/2 \pm (\omega_0^*/\omega_d) A \cos(\omega_d t + 2\gamma_0 k_w z)]\}$$
$$\times \delta[v_x \mp \omega_0^* A \sin(\omega_d t + 2\gamma_0 k_w z)]\delta[v_z \mp \omega_d A \cos(\omega_d t + 2\gamma_0 k_w z)]. \tag{93}$$

The symbol $\theta$ denotes the unit step function. This distribution function corresponds to a distribution of guiding centers that is uniform in $z$ in the region $-\infty < z < \infty$ and in $x$ in the region $-d/2 < x < d/2$.

The nonuniform fluid number density $N(x,z,t)$ which results from this distribution function is equal to $n_0$ when

$$-d/2 < x \pm (\omega_0^*/\omega_d)A\cos(\omega_d t + 2\gamma_0 k_w z) < d/2, \tag{94}$$

and is equal to zero otherwise. The nonuniform fluid velocity components $V_x(x,z,t)$ and $V_z(x,z,t)$ are equal to the right-hand sides of (90) and (91), respectively, when (94) is satisfied, and are equal to zero otherwise.

## 6. Summary and Conclusions

In this section the results of this work are summarized.

The external fields of a planar cross-field FEL [(1)] in the laboratory frame and the equations of motion of a relativistic electron in those fields [(6)-(7)] are expressed in the $\vec{E}_0^{\ell} \times \vec{B}_0^{\ell}$ drift frame moving with velocity $\vec{v}_0$ [(2)] by (5) and (10), respectively. Figure 1 shows the components of the fields in the laboratory and drift frames and the Lorentz transformation between the frames.

Two of the component equations of motion are integrated directly to yield exact invariants [(11)-(12)], which are placed into a form [(14)-(15)] suitable for the problem at hand by particular choices of the constants. The invariant equations are used, in combination with the remaining component equation of motion, to obtain a second-order differential equation for the component of electron position in the axial direction of the anode-cathode gap, $z$, as a function of time. This equation is referred to as the exact combined differential equation. [(19), supplemented by (13)-(15) and introduction of the identity $v_z = dz/dt$.] Solutions of the equation which are acceptable as a basis for the linear stability analysis

of the cross-field FEL must be periodic with the wiggler period or an integral submultiple of it when transformed into the laboratory frame. This requirement leads to a condition [(26)] which allows only the fundamental and first subharmonic resonant solutions of the exact combined differential equation.

An approximation [(40)] to the exact combined differential equation is obtained. It has the form of a weakly nonlinear oscillator that is weakly driven by a wave-harmonic excitation. It is referred to as the approximate combined differential equation. The dependent variable of this equation is a dimensionless difference, $\widetilde{\Delta z}$, [(37)] between $z$ and its guiding center, $z_0$. Its derivation involves the approximation of the quantity $\gamma^{-2}$ [(13)] by neglect of a nonresonant quantity, to yield (33), and a weakly nonlinear expansion of that approximation. It involves also a weakly nonlinear expansion of the restoring force term of (19) and neglect of nonresonant terms on the right-hand side of (40). The derivation yields a renormalized harmonic frequency $\omega_0^*$ [(36)], a dimensionless independent variable $\tilde{t}$ [(38)], a smallness parameter $\epsilon$ [(39)], and other relevant parameters [(41)-(44)].

Multiple-scale perturbation theory is used to obtain lowest-order periodic solutions of the approximate combined differential equation near the fundamental resonance. The derivation involves the introduction of fast and slow independent variables [(46)-(47), respectively], the expansion to order $\epsilon$ of the dependent variable as a function of the slow and fast variables, and the introduction of resonance conditions [(49)]. Introduction of an harmonic *ansatz* for $\widetilde{\Delta z}$ with slowly varying amplitude and phase and separation of contributions at zero and first order in $\epsilon$ yields at first order an harmonic oscillator driven by combinations of zero-order quantities [(53)]. Introduction of the resonance conditions

[(43)] and Bessel-function expansion of the wave-harmonic driving term [(55)] permits the identification of a combination of terms which drive the harmonic oscillator resonantly and therefore produce secular terms in the solution. Setting this combination of terms equal to zero and separation of real and imaginary parts yields a pair of coupled first-order differential equations [(57) and (58)] for the evolution of the slowly varying amplitude and phase. In the case of the fundamental resonance, $m = 1$, this set assumes the form (59) and (60) and the Bessel function therein can be replaced by their small-amplitude approximations. The resulting set consists of (62) and (63). Stationery solutions of (62) and (63) are obtained by setting the first-derivative terms to zero and solving the resulting algebraic equations for amplitude and phase. Two branches are obtained. The linear stability of the branches is determined by linearizing (62) and (63) about those branches. One of the branches is stable everywhere. A part of the other branch is stable. The regions of stability are shown in Figure 2.

The periodic orbits near the fundamental resonance are given in dimensional form by (79) and (82), with $A$ determined from the real, positive, root of the cubic equation (78). The orbit corresponding to the upper sign in (79) and (82) is stable for all values of the mismatch between $\omega_d$ and $\omega_0^*$. The orbit corresponding to the lower sign is stable for values of the amplitude which correspond to the condition discussed below (73). The components of particle velocity corresponding to (79) and (82) are, respectively, (80) and (81). The validity of these approximate results depend on the satisfaction of the assumptions made in obtaining them.

The approximate form of the orbits suitable for use in linearized Vlasov stability

analysis are given in (84)-(87). Vlasov distribution functions which correspond to uniform and simple nonuniform kinetic equilibria are given, respectively, in (89) and (93). The components of fluid velocity corresponding to the uniform kinetic equilibrium are given in (90) and (91). The components of fluid velocity corresponding to the uniform kinetic equilibrium are equal to the right-hand sides of (90) and (91) when the condition (94) is satisfied, and are equal to zero otherwise.


## Acknowledgements

This work was supported by the Office of Naval Research, the Air Force Office of Scientific Research, the Department of Energy, and the National Science Foundation.


## REFERENCES


1. G. Bekefi, *Appl. Phys. Lett.* **40**, 578 (1982).
2. R. C. Davidson, W. A. McMullin, and K. Tsang, *Phys. Fluids* **27**, 233 (1984).
3. C-L. Chang, E. Ott, T. M. Antonsen, Jr., and A. T. Drobot, *Phys. Fluids* **27**, 2937 (1984).
4. F. Hartemann, G. Bekefi, and R. E. Shefer, *IEEE Trans. on Plasma Science* **PS-13**, 484 (1985).
5. G. Bekefi, R. E. Shefer, and B. D. Nevins, in *Proc. Lasers '82, Soc. Optical Quantum Electron.* McLean, VA: SST Press, 1982, p. 136.
6. F. Hartemann, R. E. Shefer, and G. Bekefi, *Bull. Am. Phys. Soc.* **29**, 1283 (1984).
7. F. Hartemann, G. L. Johnston, G. Bekefi, and R. C. Davidson, *Bull. Am. Phys. Soc.* **30**, 1541 (1985).

8. F. V. Hartemann, G. L. Johnston, G. Bekefi, and R. C. Davidson, *Bull. Am. Phys. Soc.* **31**, 1540 (1985).

9. R. C. Davidson, to be published.

## FIGURE CAPTIONS

1. Electric and magnetic fields in the laboratory ($\ell$) and $\vec{E}_0^{\ell} \times \vec{B}_0^{\ell}$ drift frames, and the relation between the frames. In the figure, but not in the text, the uniform and nonuniform, time-dependent parts of the magnetic field in the drift frame have been denoted for the sake of clarity by $B_0$ and $B_w$, respectively.

2. Dimensionless mismatch $\sigma$ as a function of dimensionless amplitude $U_0$ of lowest-order periodic solution of approximate combined differential equation for fixed dimensionless amplitude $f$. Linearly stable and unstable regions of periodic solutions for stationary valules of transformed slowly-varying phase are indicated.

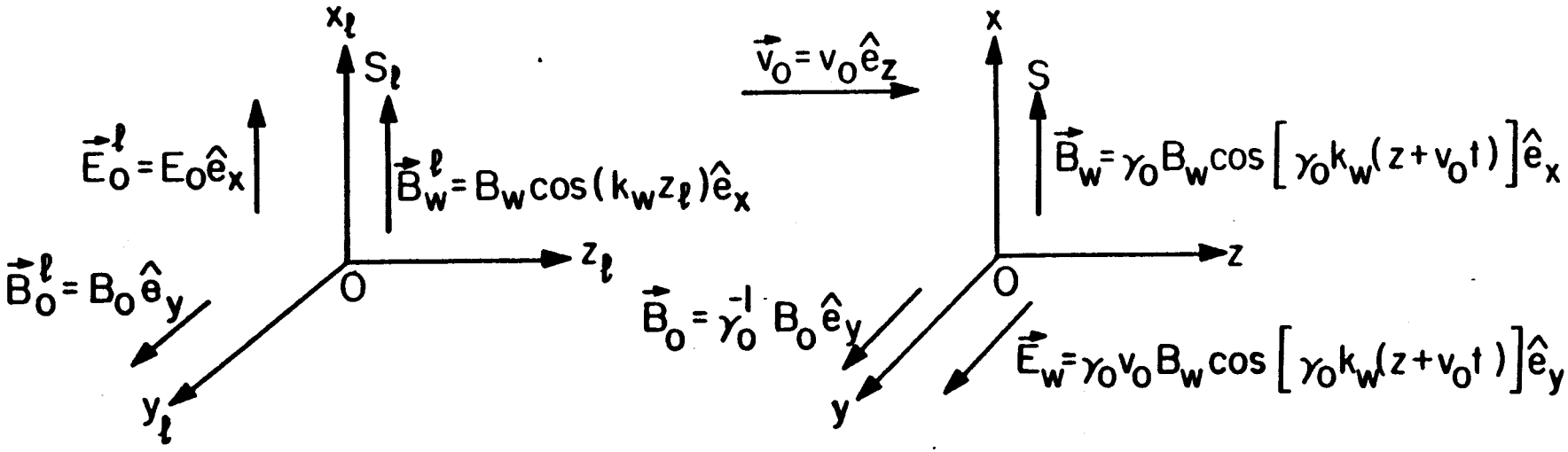
$x_\ell$
$S_\ell$
$\vec{E}_0^{\,\ell} = E_0 \hat{e}_x$
$\vec{B}_w^{\,\ell} = B_w \cos(k_w z_\ell)\hat{e}_x$
$\vec{B}_0^{\,\ell} = B_0 \hat{e}_y$
O
$z_\ell$
$y_\ell$
$\vec{v}_0 = v_0 \hat{e}_z$
x
S
$\vec{B}_w = \gamma_0 B_w \cos\left[\gamma_0 k_w (z + v_0 t)\right]\hat{e}_x$
$\vec{B}_0 = \gamma_0^{-1} B_0 \hat{e}_y$
O
z
y
$\vec{E}_w = \gamma_0 v_0 B_w \cos\left[\gamma_0 k_w (z + v_0 t)\right]\hat{e}_y$

FIGURE 1

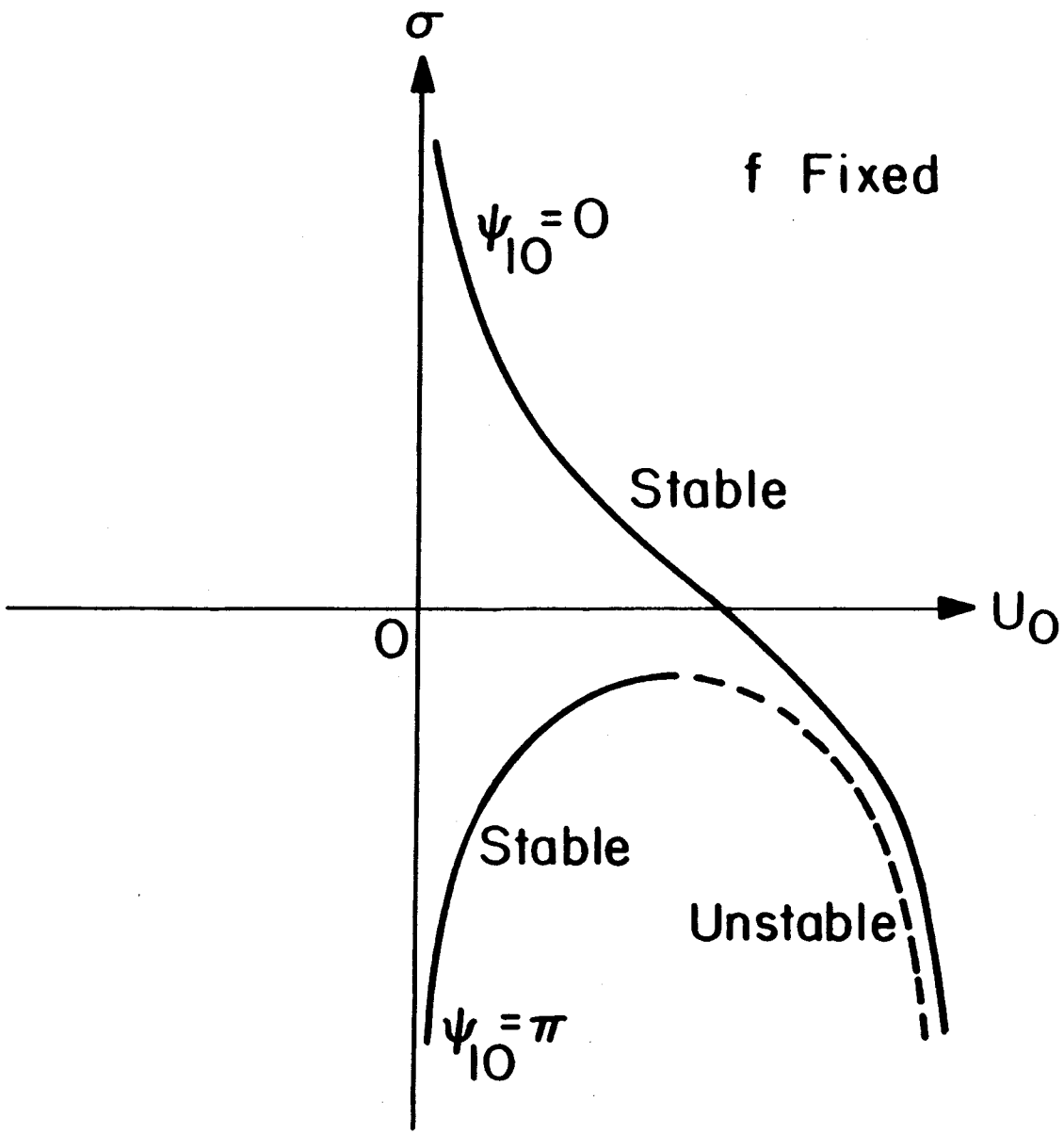


FIGURE 2